

# Effects of Rapid Quenching on the Microstructure and Electrochemical Characteristics of $\text{La}_{0.7}\text{Mg}_{0.3}\text{Co}_{0.45}\text{Ni}_{2.55-x}\text{Cu}_x$ ( $x=0\sim 0.4$ ) Electrode Alloys

Zhang Yanghuan<sup>1,2</sup>, Li Baowei<sup>2</sup>, Ren Huiping<sup>2</sup>, Wu Zhongwang<sup>2</sup>,  
Dong Xiaoping<sup>1,3</sup>, Wang Xinlin<sup>1</sup>

(1. Central Iron and Steel Research Institute, Beijing 100081, China)

(2. Inner Mongolia University of Science and Technology, Baotou 014010, China)

(3. University of Science and Technology Beijing, Beijing 100083, China)

**Abstract:** The hydrogen storage alloys  $\text{La}_{0.7}\text{Mg}_{0.3}\text{Co}_{0.45}\text{Ni}_{2.55-x}\text{Cu}_x$  ( $x = 0, 0.1, 0.2, 0.3, 0.4$ ) were prepared by casting and rapid quenching. The effects of the rapid quenching on the microstructures and electrochemical performances of the specimen alloys were investigated in detail. The results obtained by XRD, SEM and TEM show that the as-cast and quenched alloys have a multiphase structure, including the (La, Mg)Ni<sub>3</sub> phase, the LaNi<sub>5</sub> phase and the LaNi<sub>2</sub> phase. The rapid quenching has no much influence on the phase compositions of the alloys, but it obviously changed the phase abundances of the alloys. The rapid quenching can significantly improve the composition homogeneity of the alloys and markedly decrease the grain size of the alloys. The results obtained by the electrochemical measurement indicate that the rapid quenching obviously enhances the cycle stability of the alloys, but it decreases the discharge capacity and the activation capability of the alloys. The rapid quenching had an obvious influence on the discharge potential of the alloys. When the quenching rate was larger than 15 m/s, it clearly decreased the discharge plateau potential and increased the slopes of the discharge potential plateaus of the alloys.

**Key words:** La-Mg-Ni-system electrode alloy; rapid quenching; microstructures; electrochemical performances

**CLC number:** TG139.7

**Document code:** A

**Article ID:** 1002-185X(2008)06-0941-06

Science recent 30 years, a series of metal hydride electrode materials have been discovered, including the rare-earth-based  $AB_5$ -type alloys<sup>[1]</sup>, the  $AB_2$ -type Laves phase alloys<sup>[2]</sup>, the V-based solid solution alloys<sup>[3]</sup>, and the Mg-based alloys<sup>[4]</sup>. Among them,  $AB_5$ -type hydrogen storage alloy has realized large-scale industrialization in many countries, especially in Japan and China<sup>[5,6]</sup>. However, the rechargeable Ni-MH cells are encountering serious competition from Li-ion cells since  $AB_5$ -type electrode alloy as the negative electrode material in Ni-MH cell has a comparatively low capacity. Recently, Europe and major developed countries in the world issued one after the other decree for forbidding the Ni-Cd battery to be continually used, which provides a good chance for the development of the Ni-MH battery.

However, all of the currently commercialized electrode alloys, including  $AB_5$  and  $AB_2$ -types, can not meet the need of the power battery owing to their low capacities and high production costs. Therefore, finding the new type electrode alloys with higher capacity and longer cycle life becomes one of the main challenges faced by researchers in this field. Recently, several new and good hydrogen storage alloys have been reported. The most promising candidates are the La-Mg-Ni system alloys in view of their higher electrochemical capacities (360~410 mAh/g) and low production costs. However, for commercial application, the relative poor cycle stabilities of the La-Mg-Ni system alloys have to be further improved. For this purpose, the researchers in the world have carried out a lot of the investigations and obtained some

**Received date:** 2007-06-20

**Foundation items:** Supported by National High-Tech Research and Development Program of China ("863" program) (2006AA05Z132), Science and Technology Planned Project of Inner Mongolia, China (20050205) and Natural Science Foundation of Inner Mongolia, China (200711020703)

**Biography:** Zhang Yanghuan, Ph.D., Professor, Department of Functional Material Research, Central Iron and Steel Research Institute, Beijing 100081, P. R. China, Tel: 0086-010-62187570; E-mail: zyh59@yahoo.com.cn

important results<sup>[7~10]</sup>. It is well known that the element substitution is one of the effective methods for improving the overall properties of the hydrogen storage alloys<sup>[11,12]</sup>, and the preparation technology is extremely important for improving the performances of the alloys. Therefore, it is expected that an alloy with high discharge capacity and good cycling stability may be produced by an optimized amount of Cu substitution in La-Mg-Ni system alloy and a selected rapid quenching technique. Therefore, in this paper a systematic investigation on the effects of the rapid quenching on the microstructures and the electrochemical performances of the  $\text{La}_{0.7}\text{Mg}_{0.3}\text{Co}_{0.45}\text{Ni}_{2.55-x}\text{Cu}_x$  ( $x=0\sim 0.4$ ) electrode alloys was made.

## 1 Experimental Methods

The experimental alloys were melted in an argon atmosphere in a vacuum induction furnace. The purity of all the component metals (La, Ni, Co, Mg and Cu) was 99.8% at least. A binary La-Mg intermediate alloy (30%Mg+70%La) was beforehand prepared by electrolytic synthesis and a positive argon pressure of 0.1 MPa was applied for preventing the volatilization of magnesium during melting. After induction melting, the melt was poured into a copper water cooled mould, and a cast ingot was obtained. Part of the as-cast alloys was re-melted and quenched by melt-spinning with a rotating copper wheel. The quenching rate was expressed by the linear velocity of the copper wheel and the quenching rates used in the experiment were 15, 20, 25 and 30 m/s, respectively. The nominal composition of the investigated alloys was  $\text{La}_{0.7}\text{Mg}_{0.3}\text{Co}_{0.45}\text{Ni}_{2.55-x}\text{Cu}_x$  ( $x = 0, 0.1, 0.2, 0.3, 0.4$ ). Corresponding with Cu content, the alloys were denoted by  $\text{Cu}_0, \text{Cu}_1, \text{Cu}_2, \text{Cu}_3$  and  $\text{Cu}_4$ , respectively.

The phase structures and compositions of the alloys were determined by XRD diffractometer of D/max/2400. The diffraction was performed with  $\text{Cu K}\alpha_1$  radiation filtered by graphite. The experimental parameters for determining phase structure were 160 mA, 40 kV and  $10^\circ/\text{min}$ , respectively. The polished samples were etched with a 60% HF solution, and the morphologies and the micro-zone compositions of the alloys were examined by SEM. The powder samples were dispersed in anhydrous alcohol for observing the grain morphology with transmission electron microscopy (TEM), and the crystalline state of the specimen was determined with selected area electron diffraction (SAD).

Round electrode pellets with 15 mm in diameter were prepared by mixing 1 g of alloy powder with fine nickel powder in a mass ratio of 1:1 together with a

small amount of polyvinyl alcohol (PVA) solution as binder, and then compressed under a pressure of 35 MPa. After drying for 4 h, the electrode pellets were immersed in a 6 mol/L KOH solution for 24 h in order to wet the electrodes fully before the electrochemical measurement.

The experimental electrodes were tested in a tri-electrode open cell, consisting of a metal hydride working electrode, a  $\text{NiOOH}/\text{Ni}(\text{OH})_2$  counter electrode and a  $\text{Hg}/\text{HgO}$  reference electrode. The electrolyte was a 6 mol/L KOH solution. The voltage between the negative electrode and the reference electrode is defined as the discharge voltage. In every cycle, the alloy electrode was charged with a constant current of 100 mA/g for 5 h, after resting 15 min, it was then discharged at 100 mA/g to a  $-0.500$  V cut-off voltage. The environment temperature of the measurement was kept at  $30^\circ\text{C}$ .

## 2 Results and Discussion

### 2.1 Effect of rapid quenching on the microstructure

The XRD patterns of the as-cast and quenched  $\text{Cu}_2$  alloy were shown in Fig.1. It can be seen in Fig.1 that the as-cast and quenched alloys exhibited a multiphase structure, composed of the  $(\text{La, Mg})\text{Ni}_3$ , the  $\text{LaNi}_5$  and the  $\text{LaNi}_2$  phases. The rapid quenching did not have great influence on the phase composition of the alloy, but it obviously changed the phase abundance of the alloy. Rapid quenching reduced the amount of  $\text{LaNi}_2$  phase in the  $\text{Cu}_2$  alloy. The lattice parameters of the  $\text{LaNi}_5$  and  $(\text{La, Mg})\text{Ni}_3$  main phases in the as-cast and quenched  $\text{Cu}_2$  alloy, which were calculated from the XRD data by a software of Jade 6.0, are listed in Table 1. The results indicate that the rapid quenching leads to the increase of  $c$  axis and the slight decrease of  $a$  axis and cell volume of the  $\text{LaNi}_5$  and  $(\text{La, Mg})\text{Ni}_3$  main phases.

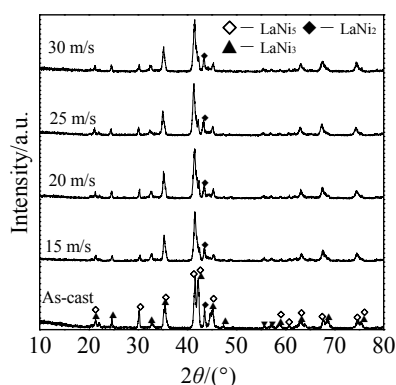


Fig.1 The X-ray diffraction patterns of the as-cast and quenched  $\text{Cu}_2$  alloy

The morphologies of the as-cast and quenched  $\text{Cu}_2$  alloy were inspected by SEM, as shown in Fig.2. The results indicate that the as-cast and quenched alloys were

of multiphase structure, containing both the  $(\text{La, Mg})\text{Ni}_3$  and the  $\text{LaNi}_5$  phases. Because the amount of the  $\text{LaNi}_5$  phase was small and it attached the  $(\text{La, Mg})\text{Ni}_3$  phase in the process of growing, it is difficult to see the morphology of the  $\text{LaNi}_5$  phase. It can be seen from Fig.2a that the grains of the as-cast alloy were very coarse and the composition homogeneity was very poor. Comparing with the morphologies of the as-cast alloys, the rapid quenching markedly refined the grains and significantly improved the composition homogeneity of the alloys, and the grain sizes of the as-quenched alloy shortened with increasing of quenching rate. The morphologies and the crystalline state of the as-quenched  $\text{Cu}_0$  and  $\text{Cu}_2$  alloys were examined by TEM, as shown in Fig.3. Fig.3 displays that  $\text{Cu}_0$  alloy had a clear crystal characteristic, but  $\text{Cu}_2$  alloy showed a like amorphous

one. This indicates that the substitution of Cu for Ni is favourable to the formation of an amorphous phase.

**Table 1** Lattice parameters and cell volume of the  $\text{LaNi}_5$  and  $(\text{La, Mg})\text{Ni}_3$  main phases for the as-cast and quenched  $\text{Cu}_2$  alloy

Alloy states	Main phase	Lattice constant/nm		Cell volume/ $\text{nm}^3$
		<i>a</i>	<i>c</i>	
As-cast	$(\text{La, Mg})\text{Ni}_3$	0.506	2.4324	0.5393
	$\text{LaNi}_5$	0.5036	0.4051	0.089
15 m/s	$(\text{La, Mg})\text{Ni}_3$	0.5058	2.4331	0.539
	$\text{LaNi}_5$	0.5033	0.4055	0.089
20 m/s	$(\text{La, Mg})\text{Ni}_3$	0.5055	2.4341	0.5386
	$\text{LaNi}_5$	0.5031	0.4057	0.0889
25 m/s	$(\text{La, Mg})\text{Ni}_3$	0.5048	2.4349	0.5373
	$\text{LaNi}_5$	0.5026	0.4060	0.0888
30 m/s	$(\text{La, Mg})\text{Ni}_3$	0.5041	2.4352	0.5359
	$\text{LaNi}_5$	0.5021	0.4064	0.0887

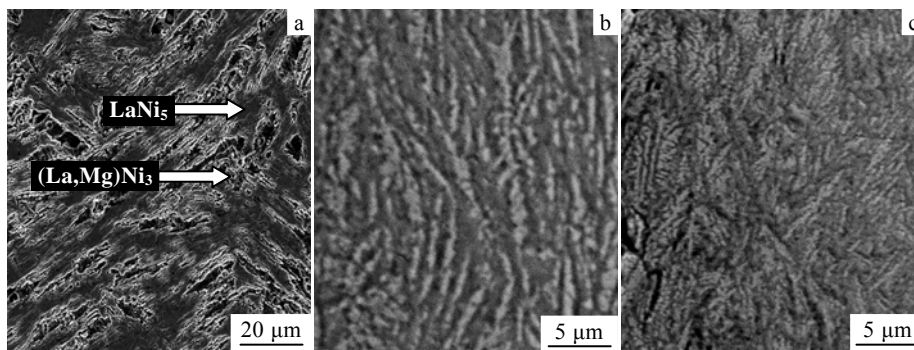


Fig.2 SEM morphologies of the  $\text{Cu}_2$  alloy: (a) as-cast, (b) 15 m/s, and (c) 30 m/s

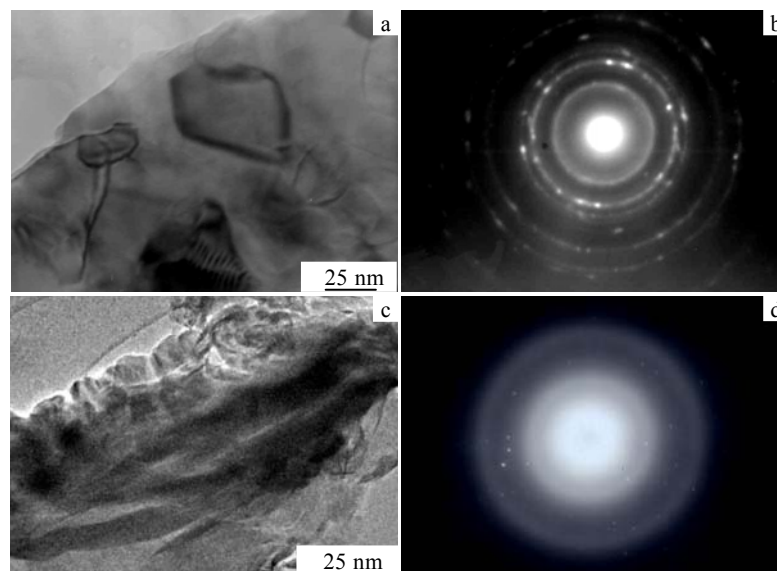


Fig.3 The morphology and SAD of the as-quenched (30 m/s)  $\text{Cu}_0$  and  $\text{Cu}_2$  alloys taken by TEM (a) and (b) morphology and SAD of  $\text{Cu}_0$  alloy; (c) and (d) morphology and SAD of  $\text{Cu}_2$  alloy

## 2.2 Effect of rapid quenching on the electrochemical performance

### 2.2.1 Discharge capacity

The discharge capacities of the alloys as a function

of the quenching rate are shown in Fig.4, and the charge-discharge current density is 100 mA/g. It is clear to see that an increase of the quenching rate means an obvious decrease of the discharge capacity of the alloys with a fixed alloy. When the quenching rate increased from 0 (As-cast is defined as quenching rate of 0 m/s) to 30 m/s, the capacity of Cu<sub>0</sub> alloy decreased from 396.4 to 364.6 mAh/g, and that of Cu<sub>4</sub> alloy from 382.4 to 349.1 mAh/g. The discharge capacity of the alloy is relevant to its crystal structure, phase composition and structure, grain size, composition homogeneity and surface state. The influence of rapid quenching on the capacity is complicated. Both the improvement of the composition homogeneity and the decrease of the grain size of the alloys as result of rapid quenching are favourable for the capacity on one hand, but the increase of the lattice stress is unfavourable on the other hand<sup>[13]</sup>. Therefore, whether rapid quenching would increase or decrease the capacity of the alloy depends on the relative predominance of the above effects. The lattice stress and an amorphous phase are mainly responsible for the capacity of the alloys which decreases with increasing of quenching rate because the discharge capacity of an amorphous phase is about half as large as that of the crystalline alloy<sup>[14]</sup>.

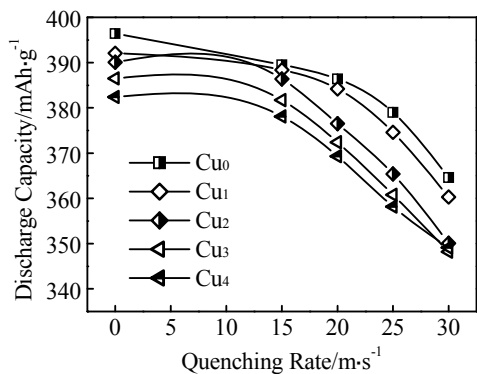


Fig.4 Evolution of the discharge capacity of the alloys with the quenching rate

### 2.2.2 High rate discharge capability (HRD)

The high rate discharge ability (HRD) determining mainly the kinetic property of the hydrogen storage alloy electrode is defined and calculated according to the following formula:  $HRD = C_{600}/C_{100} \times 100\%$ , where  $C_{600}$  is the discharge capacity of the electrode discharged at the current density of 600 mA/g, and  $C_{100}$  is the discharge capacity measured at a discharge current density of 100 mA/g. The quenching rate dependence of the HRDs of the alloys is illustrated in Fig.5. The figure exhibits that the rapid quenching has different influences on the HRDs of the alloys. The HRD of the Cu-free alloy

had a maximum value with variety of the quenching rate, but the HRDs of the alloys containing Cu monotonously decreased with the incremental change of the quenching rate. The decisive factor of the alloy's HRD is the diffusion capability of the hydrogen atoms in the alloy. The grain refinement produced by rapid quenching is favourable for improving the HRD of the alloy because the grain boundaries provide good diffusion tunnel for the diffusion of the hydrogen atoms, but an amorphous phase is unfavourable for it. For Cu-free alloy, the influence of the grain refinement was dominating when quenching rate was less than 15 m/s. Increasing quenching rate over 15 m/s, a negative function of an amorphous phase became stronger. Therefore, the HRD of the Cu<sub>0</sub> alloy had a maximum value with the variety of the quenching rate. The substitution of Cu expedited the formation of an amorphous phase, which led to a monotonous decrease of the containing Cu alloys' HRDs with the variety of the quenching rate.

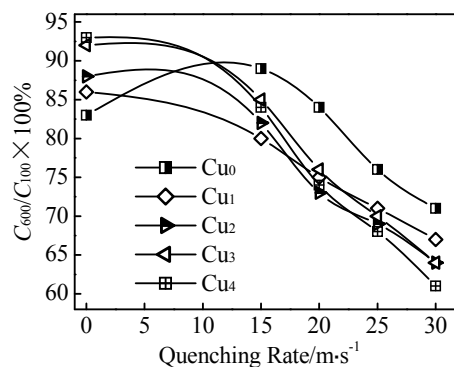


Fig.5 Evolution of the HRD of the alloys with the quenching rate

### 2.2.3 Discharge potential characteristic

The discharge potential characteristic characterized by the potential plateau of the discharge potential curve of the alloy is an important performance of the electrode alloy. The longer and the more horizontal the discharge potential plateau, the better the discharge characteristic of the alloy. The discharge potential curves of the as-cast and quenched Cu<sub>2</sub> alloy are shown in Fig.6. The rapid quenching had a clear influence on the discharge potential of the alloy, and led to a melioration of the plateau characteristic of the discharge potential curves when quenching rate was  $\leq 15$  m/s. When the quenching rate was larger than 15 m/s, it notably decreased the discharge plateau potential and raised the slopes of the discharge potential plateaus of the alloy. Generally, the plateau potential is closely relative to the internal resistance of the battery, including ohmic internal resistance and polarization resistance. The discharge reaction of the hydrogen storage electrode

mainly depends on the diffusion of hydrogen atoms in the alloy, and internal resistance of the alloy electrode reduces with the increase of the diffusion coefficient of the hydrogen atom<sup>[15]</sup>. The substitution of Cu leads to a sharp reduction of the diffusion coefficient of the hydrogen atom, for which the amorphous phase and the oxidation layer on the surface of the alloy electrode are mainly responsible. Therefore, it seems to be self-evident that the substitution of Cu impaired the discharge potential characteristics of the alloys.

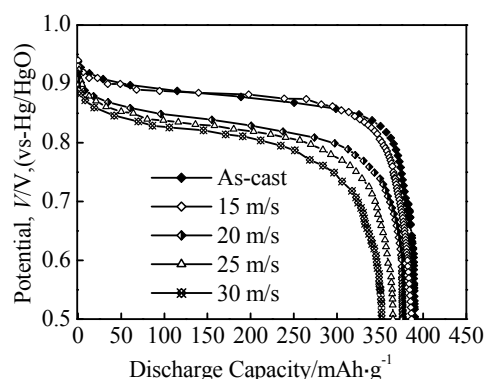


Fig.6 The discharge potential curves of the as-cast and quenched  $\text{Cu}_2$  alloys

#### 2.2.4 Cycle life

The cycle life, indicated by  $N$ , is characterized by the cycle number. The quenching rate dependence of the cycle life of the alloys is presented in Fig.7. It can be seen in Fig.7 that the cycle lives of the alloys prolonged with the increase of the quenching rate. When the quenching rate increased from 0 to 30 m/s, the cycle lives of  $\text{Cu}_0$  alloy increased from 81 to 105 cycles and that of the  $\text{Cu}_4$  alloy from 97 and 131 cycles.

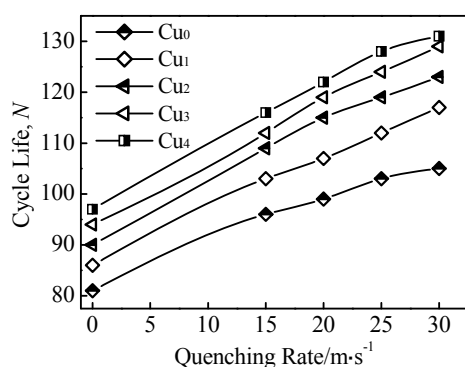


Fig.7 Change of the cycle life of the alloys with the quenching rate

The cycle stability of electrode alloy is an overwhelming factor of the life of Ni-MH battery. The root cause of leading to battery lose efficacy is on

negative electrode rather than on positive electrode. The result in the literatures<sup>[16,17]</sup> confirmed that the fundamental reasons for the capacity decay of the electrode alloy are the pulverization and oxidation of the alloy during charge-discharge cycle. The rapid quenching significantly enhanced the anti-pulverization capability and the cyclic stability of the alloy in virtue of the grain refinement and the formation of an amorphous phase. The smaller the grain size, the stronger the anti-pulverization capability, and an amorphous phase can increase not only the anti-pulverization ability but also the anti-corrosion capability of the alloy<sup>[18]</sup>.

### 3 Conclusions

1) Rapid quenching has no much influence on the phase compositions of the  $\text{La}_{0.7}\text{Mg}_{0.3}\text{Co}_{0.45}\text{Ni}_{2.55-x}\text{Cu}_x$  ( $x = 0, 0.1, 0.2, 0.3, 0.4$ ) alloys, but it obviously changes the phase abundances of the alloys. Rapid quenching leads to a slight increase of  $c$  axis and an imperceptible decrease of  $a$  axis and cell volume of structural data of the alloys, and it significantly improves the composition homogeneity and markedly decreases the grain size of the alloy.

2) The rapid quenching clearly enhances the cycle stability of the alloys, but the discharge capacity of the alloys decreases with the increase of the quenching rate. The  $HRD$  of the Cu-free alloy has a maximum value with variety of the quenching rate, but the  $HRDs$  of the alloys containing Cu monotonously decreases with the incremental change of the quenching rate. The influence of rapid quenching on the discharge potential characteristic of the alloy is changeable with the variety of the quenching rate. When quenching rate was  $\leq 15$  m/s, rapid quenching leads to the melioration of the plateau characteristic of the discharge potential curves. But when the quenching rate is larger than 15 m/s, it notably decreases the discharge plateau potential and raises the slopes of the discharge potential plateaus of the alloy.

### References

- [1] Willems J J G, Buschow K H J. *J Less-Common Met*[J], 1987, 129: 13
- [2] Ovshinsky S R, Fetcenko M A, Ross J. *Science*[J], 1993, 260: 176
- [3] Tsukahara M, Kamiya T, Takahashi K *et al.* *J Electrochem Soc* [J], 2000, 147: 2941
- [4] Sun D L, Enoki H, Gingl F *et al.* *J Alloys Compd*[J], 1999, 285(2): 279
- [5] Uehara I, Sakai T, Ishikawa H. *J Alloys Compd*[J], 1997,

- 253-254: 635
- [6] Wang Q D, Chen C P, Lei Y Q. *J Alloys Compd*[J], 1997, 253~254: 629
- [7] Kohno T, Yoshida H, Kawashima F *et al.* *J Alloys Compd*[J], 2000, 311(2): L5
- [8] Kadir K, Uehara I, Sakai T. *J Alloys Compd*[J], 1997, 257(1-2): 115
- [9] Pan H G, Liu Y F, Gao M X *et al.* *J Electrochem Soc*[J], 2003, 150(5): A565
- [10] Liao B, Lei Y Q, Chen L X *et al.* *J Power Sources*[J], 2004, 129(2): 358
- [11] Akito Takasaki, Kazuya Sasao. *J Alloys Compd*[J], 2005, 404~406: 431
- [12] Reilly J J G, Besenhard J O. *Handbook of Battery Materials* [M]. New York: Wiley, 2000
- [13] Zhang Y H, Wang G Q, Dong X P *et al.* *J Power Sources*[J], 2005, 148: 105
- [14] Li Y, Cheng Y T. *J Alloys Compd*[J], 1995, 223: 6
- [15] Lai Weihua(赖为华), Yu Chengzhou(余成洲). *Battery*(电池)[J], 1996, 26(4): 189
- [16] Chartouni Daniel, Meli Felix, Züttel Andreas *et al.* *J Alloys Compd*[J], 1996, 241: 160
- [17] Sakai, Oguro K, Miyamura H *et al.* *J Less-Common Met*[J], 1990, 161(2): 193
- [18] Zhang Y H, Wang G Q, Dong X P *et al.* *J Alloys Compd*[J], 2004, 379: 298

## 快淬对 $\text{La}_{0.7}\text{Mg}_{0.3}\text{Co}_{0.45}\text{Ni}_{2.55-x}\text{Cu}_x$ ( $x = 0-0.4$ ) 电极合金微观结构及电化学性能的影响

张羊换<sup>1,2</sup>, 李保卫<sup>2</sup>, 任慧平<sup>2</sup>, 吴忠旺<sup>2</sup>, 董小平<sup>1,3</sup>, 王新林<sup>1</sup>

(1. 钢铁研究总院, 北京 100081)

(2. 内蒙古科技大学, 内蒙古 包头 014010)

(3. 北京科技大学, 北京 100083)

**摘要:** 应用铸造及快淬工艺制备了  $\text{La}_{0.7}\text{Mg}_{0.3}\text{Co}_{0.45}\text{Ni}_{2.55-x}\text{Cu}_x$  ( $x = 0, 0.1, 0.2, 0.3, 0.4$ ) 贮氢电极合金, 研究了快淬工艺对合金微观结构及电化学性能的影响。XRD, SEM 及 TEM 的分析结果表明, 铸态及快淬态合金具有多相结构, 包括 (La, Mg)Ni<sub>3</sub> 相, LaNi<sub>5</sub> 相以及 LaNi<sub>2</sub> 相。快淬对合金的相组成没有明显影响, 但显著地改变了合金的相丰度。快淬还显著地改善合金的成分均匀性, 并使合金的晶粒明显细化。电化学测试的结果表明, 快淬大幅度提高合金的电化学循环稳定性, 但使合金的放电容量和活化性能下降。快淬对合金的放电电压特性具有明显的影响, 当淬速大于 15 m/s 时, 快淬降低合金的放电电压, 并使放电平台的斜率明显增大。

**关键词:** La-Mg-Ni 系电极合金; 快淬; 微观结构; 电化学性能

作者简介: 张羊换, 男, 1959 年生, 博士, 教授, 钢铁研究总院功能材料研究所, 北京 100081, 电话: 010-62187570, E-mail: zyh59@yahoo.com.cn